International Forum of Allergy & Rhinology

WILEY

ORIGINAL ARTICLE OPEN ACCESS

Healing Following Endoscopic Reconstruction of the Anterior Skull Base in Patients With Sinonasal Malignancies

Giacomo Contro[1] | Leonardo Calvanese[2] | Piergiorgio Gaudioso[1] | Stefano Taboni[1] | Mosè Sozzi[3] | Gloria Schiavo[4] | Alessandra Sordi[5] | Isabelle Dohin[6] | Francesca Mularoni[7,8] | Giuseppe Roccuzzo[9] | Ester Orlandi[10,11] | Barbara Vischioni[10] | Gianluca Dalfino[4] | Carlotta Pessina[12] | Roberto Maroldi[13] | Mario Turri-Zanoni[4] | Cesare Piazza[6,14] | Paolo Battaglia[4] | Maurizio Bignami[15] | Paolo Castelnuovo[4] | Davide Mattavelli[6,14] | Piero Nicolai[1] | Marco Ferrari[1]

[1]Section of Otorhinolaryngology-Head and Neck Surgery, Department of Neuroscience (DNS), University of Padova, Padova, Italy | [2]ENT Unit, Surgical Department, Ospedali Riuniti Padova Sud, Monselice-Padova, Italy | [3]Otolaryngology Unit, S. Valentino Hospital, Montebelluna (TV), AULSS2 Marca Trevigiana, Italy | [4]Department of Otolaryngology Head and Neck Surgery, ASST Lariana, Ospedale Sant'Anna, University of Insubria, Como, Italy | [5]Unit of Otorhinolaryngology, ASST del Garda, Manerbio Hospital, Manerbio, Italy | [6]Unit of Otorhinolaryngology–Head and Neck Surgery, ASST Spedali Civili di Brescia, Brescia, Italy | [7]Division of Head and Neck Surgery, Department of Surgery, The University of Hong Kong, Queen Mary Hospital, Hong Kong, China | [8]ENT Department, Head Neck Cancer Unit, San Giovanni Bosco Hospital, Turin, Italy | [9]Department of Otorhinolaryngology–Head and Neck Surgery, Liverpool University Hospitals NHS Foundation Trust, Liverpool, UK | [10]Radiation Oncology Unit, Clinical Department, CNAO National Center for Oncological Hadrontherapy, Pavia, Italy | [11]Department of Clinical, Surgical, Diagnostic and Pediatric Sciences, University of Pavia, Pavia, Italy | [12]Radiology Unit, Sant'Antonio Hospital, University of Padova, Padova, Italy | [13]Radiology Unit, ASST Spedali Civili di Brescia, University of Brescia, Brescia, Italy | [14]Department of Medical and Surgical Specialties, Radiological Sciences, and Public Health University of Brescia, Brescia, Italy | [15]Division of Otorhinolaryngology, Department of Biotechnology and Life Sciences, University of Insubria, ASST Sette Laghi Hospital, Varese, Italy

Correspondence: Marco Ferrari (marco.ferrari@unipd.it)

Received: 22 May 2026 | **Revised:** 10 July 2026 | **Accepted:** 19 July 2026

Keywords: adjuvant radiotherapy | anterior skull base reconstruction | endoscopic endonasal surgery | endoscopic healing | iliotibial tract graft

ABSTRACT

Background: Healing dynamics after anterior skull base (ASB) reconstruction following transnasal endoscopic surgery (TES) for sinonasal malignancies remain poorly characterized. This study aimed to describe the postoperative healing process, quantify time to healing, identify factors influencing healing, and assess radiologic evolution over time.

Methods: This multicenter retrospective study included adult patients undergoing TES with craniectomy and ASB reconstruction for sinonasal malignancies between 2016 and 2024. Serial endoscopic examinations were reviewed using a novel stage-based classification system. Postoperative contrast-enhanced magnetic resonance imaging (MRI) was analyzed to evaluate reconstruction layers, enhancement patterns, thickness changes, and brain sagging. Cumulative incidence analysis, multistate modeling, and uni- and multivariable analyses were performed to identify factors associated with healing.

Results: A total of 173 patients were included. Complete endoscopic healing was achieved in 15.9% of patients at 6 months, 69.9% at 12 months, and 94.4% at 24 months. Local pedicled flap reconstruction was associated with faster healing, with complete healing achieved in 89.4% of patients at 12 months compared with 60.7% in graft-based reconstructions ($p < 0.001$). Adjuvant radiotherapy (RT), particularly intensity-modulated proton therapy, was independently associated with delayed healing. MRI showed progressive reduction in reconstruction thickness, decreased visibility of adipose tissue and the outer graft layer, and increased brain sagging over time. RT was associated with greater remodeling changes, whereas flap-based reconstruction appeared to mitigate these effects.

Conclusions: Healing after ASB reconstruction following TES is a prolonged and dynamic process influenced mainly by reconstruction technique and adjuvant RT. Local vascularized flaps promote faster and more stable healing and may be particularly advantageous in patients requiring postoperative RT.

1 | Introduction

Transnasal endoscopic surgery (TES) has progressively become the mainstay of treatment for sinonasal cancers that require surgery, and craniectomy with dural resection is indicated if the tumor is in close contact or crosses the anterior skull base (ASB) [1–4]. A watertight reconstruction of the ASB that separates the intracranial compartment from the sinonasal cavities is essential to prevent cerebrospinal fluid (CSF) leak and its potentially life-threatening complications. Tissue remodeling after skull base repair depends on the integration of the different layers of reconstruction, which is one of the key concerns in achieving tight dural closure [5]. An effective option for ASB reconstruction is the three-layer iliotibial tract (ITT) technique, owing to its favorable characteristics of thickness, strength, and pliability [4–8]. When the tumor does not extend contralaterally and the nasal septum is uninvolved, local pedicled flaps can be harvested to reduce the probability of postoperative CSF leaks and to promote rapid healing of the surgical cavity, with reduced crusting and nasal discharge [9].

Several studies have analyzed possible factors associated with prolonged healing time and failure of ASB reconstructions: (i) size of the defect [10, 11], (ii) anatomical site of the defect and whether the borders of the defect can be identified and exposed, [12] (iii) presence and flow of intraoperative CSF leaks [13, 14], (iv) surgical techniques (grafts vs. vascularized flaps) [15], and (v) adjuvant radiotherapy (RT) [10, 16, 17]. To the best of our knowledge, no clear evidence is available on the timing of healing of ASB reconstructions after TES with dural resection. Moreover, there is limited evidence regarding the variables that affect the healing process, and no consensus exists on how to define and classify the different stages of the healing process after endoscopic resection with transnasal craniectomy (ERTC). The primary objectives of this study were to (i) define the endoscopic phases of healing of ASB reconstruction through a novel classification system and (ii) quantify the time required to achieve complete healing. The secondary objective was to identify clinical, surgical, and adjuvant treatment-related factors associated with the healing process. In addition, postoperative magnetic resonance imaging (MRI) findings were analyzed to characterize the radiological evolution of the reconstruction over time.

2 | Materials and Methods

The study included adult patients undergoing ERTC with curative intent and a reconstruction of the ASB for nasoethmoidal malignancies from January 1, 2016, to December 31, 2024. The institutional database on sinonasal cancers of (a) the Section of Otorhinolaryngology–Head and Neck Surgery of the University of Padova (Padova, Italy), (b) the Unit of Otorhinolaryngology–Head and Neck Surgery, ASST Spedali Civili of Brescia—University of Brescia (Brescia, Italy), (c) the Division of Otorhinolaryngology-Head and Neck Surgery, University of Insubria (Varese and Como, Italy) was retrospectively analyzed. Patients who received previous surgery involving the ASB and those missing both endoscopic and radiologic evaluations were excluded from the analysis. The study was conducted according to the ethical standards established in the Declaration of Helsinki. Retrospective research on patients with sinonasal cancers was approved by local ethics committees of the Centers involved in the study: (i) Comitato Etico per la Sperimentazione Clinica della Provincia di Padova, protocol no. 433n/AO/23; (ii) Comitato Etico ASST Spedali Civili, protocol no. 3616; (iii) Comitato Etico Ospedale di Circolo e Fondazione Macchi, code: 0033025/2015; and (iv) Comitato Etico ASST Lariana, protocol no. 212/2024.

2.1 | Dural Repair Technique

In our Institutions, dural reconstruction following ERTC is performed according to a standardized, defect-driven algorithm based on the extent of resection and availability of vascularized flaps. When the nasal septum is not available due to tumor involvement, a three-layer reconstruction using ITT grafts is routinely adopted, consisting of (i) an intradural layer, (ii) an intracranial extradural layer, and (iii) an extracranial layer to achieve a watertight closure [4]. Autologous fat is interposed between the second and third layers along the margins of the reconstruction to obliterate dead spaces and enhance sealing. In cases of bilateral craniectomy where the inferior portion of the contralateral septum can be preserved, multilayer ITT reconstruction is combined with a posteriorly based nasoseptal flap used as the outermost layer. For unilateral defects, reconstruction is typically achieved using autologous or heterologous grafts in combination with a septal flip flap, allowing effective mucosal resurfacing of the skull base [9, 18]. For study purposes, patients were categorized according to the presence or absence of a local vascularized flap, since all reconstructions shared the same multilayer graft-based foundation. When available and deemed adequate to the defect size and characteristics, a collagen matrix was used instead of the ITT layers to avoid donor site morbidity.

2.2 | Data Collection

Demographic and clinical data, including information on previous treatment, histology (defined in accordance with the fourth edition of WHO Classification of Head and Neck Tumors) [19], pre- and post-operative images, TNM classification (eighth edition), [20] surgical reports, size of the defect, margin status,

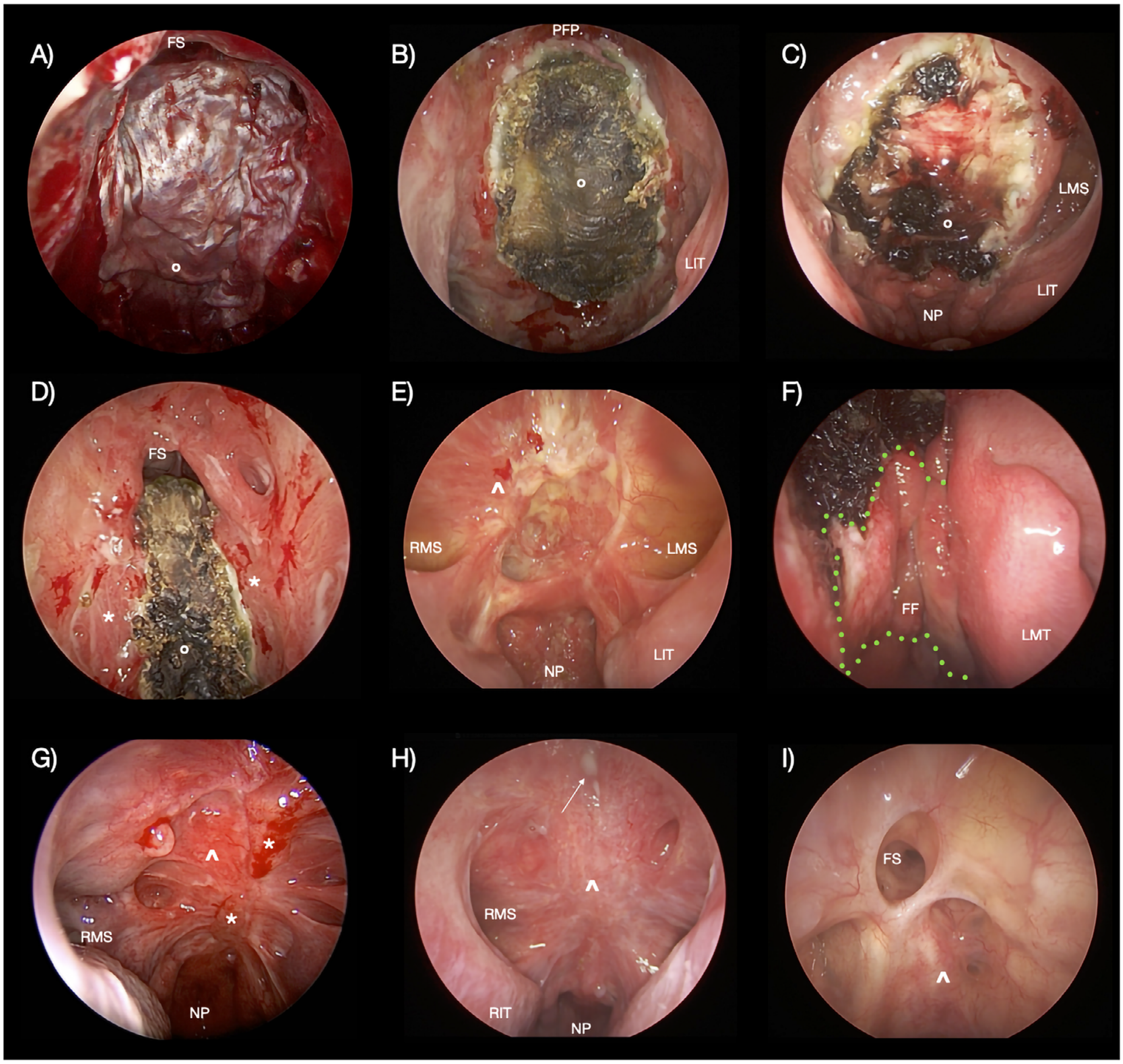

FIGURE 1 | Endoscopic classification of the healing of the anterior skull base reconstruction. Healing grade varies from phase 1, postoperative, to phase 6, complete recovery.FS: frontal sinus; PFP: posterior frontal plate; LIT: left inferior turbinate; RIT: right inferior turbinate; LMS: left maxillary sinus; RMS: right maxillary sinus; NP: nasopharynx; LMT: left middle turbinate; FF: flip flap; o: third layer of the iliotibial tract; *: granulation tissue; ^: mucosa; white arrow: stenosis with purulent secretion of the frontal sinusotomy.

complications, adjuvant treatments, and follow-up data, were retrieved with medical chart review.

2.3 | Endoscopic Classification

Endoscopic follow-up videos were retrospectively analyzed. The healing status of the ASB reconstruction and the surrounding sinonasal cavity was classified as follows:

1. *Phase 1*: The reconstruction of the ASB as it appears at the end of surgery: the third layer of ITT is evident and has its native appearance (Figure 1A).
2. *Phase 2*: Integration or necrosis of the third layer of ITT (necrosis can appear as either desiccation or colliquation or a combination of the two). Gentle manipulation of the ITT (necrotized—Figure 1B, or integrated—Figure 1C) confirms graft stability with respect to the underlying tissues.
3. *Phase 3*: It includes formation of granulation tissue. The second or third layer of ITT is still visible, and granulation tissue develops from the edges of the plasty, starting to cover the graft (Figure 1D).
4. *Phase 4a*: The ASB reconstruction is completely covered by granulation tissue. The ITT is no longer visible; at the edges of the defect, mucosa starts to replace the granulation area (Figure 1E).

5. *Phase 4b*: The ASB reconstruction is mostly covered by mucosa. Granulation tissue and/or areas of bone/cartilage exposure can still be appreciated in the sinonasal cavity surrounding the ASB reconstruction. This grade was assigned to the first endoscopic evaluation of ASB reconstructions with local flaps (Figure 1F), unless there was necrosis of the flap.
6. *Phase 5*: The ASB reconstruction is completely covered by mucosa. No areas of bony/cartilaginous exposure are visible; granulation or non-integrated mucosa edges are appreciable (Figure 1G).
7. *Phase 6a*: The sinonasal cavity is entirely covered by mucosa. No areas of bony/cartilaginous exposure, granulation, or non-integrated mucosa edges are appreciable; at least one of the following findings was present: (1) areas of edema, (2) crusting with purulent secretions, and (3) stenotic sinusotomy (Figure 1H).
8. *Phase 6b*: The sinonasal cavity is entirely covered by mucosa. No areas of bony/cartilaginous exposure, granulation, non-integrated mucosa edges, edema, crusting with purulent secretions, or stenotic sinusotomy are appreciable (Figure 1I).

Healing phases were grouped into three stages: stage 1 corresponded to phase 1 (i.e., the "postoperative stage"), stage 2 grouped together phases 2, 3, 4a and 4b (i.e., the "healing stage," characterized by an ongoing healing process), and stage 3 included phases 5, 6a and 6b (i.e., the "complete healing stage," where the healing process is completed). Transitions in the various stages were defined as follows: *transition 1* indicated the transition from stage 1 ("postoperative") to stage 2 ("healing"), referring to the initiation of the healing process; *transition 2* indicated the transition from stage 1 ("postoperative") to stage 3 ("complete healing"), referring to a very rapid healing process (no evidence of stage 2 at the endoscopic evaluations), and *transition 3* indicated the transition from stage 2 ("healing") to stage 3 ("complete healing"), referring to a healing process with clinical evidence of intermediate healing phases at outpatient endoscopic evaluations.

2.4 | Radiological Evaluation

Postoperative contrast-enhanced MRIs were retrospectively analyzed. MRIs without contrast agent or with a section thickness of ≥3 mm were excluded from the following analyses. The following radiological features were assessed (Figure 2): visualization of the first and second layers, their vascularization (defined as evidence of contrast enhancement), visualization of the fat and third layer, the minimum thickness of the ASB reconstruction, measured on the sagittal plane, the presence or absence of a layer of contrast-enhanced endonasal tissue (and its thickness), and brain sagging. The last feature was evaluated in the coronal plane passing through the origin of the optic nerves, posterior to the eyeball, using as a reference the line tangent to the upper margins of the superior oblique muscles.

3 | Statistical Analysis

RStudio (version 4.3.1, https://rstudio.com/) was used for statistical analysis. The description of the healing process was performed using a unidirectional multistate model, analyzing the transition through healing stages as a function of time.

Inter- and intra-rater reliability of the endoscopic healing classification was assessed by calculating Krippendorff's alpha for overall agreement among raters (G.C., P.G., S.T., and G.R.) and weighted Cohen's kappa coefficients for pairwise inter-rater and intra-rater agreement.

The inferential analysis of the factors influencing the healing process was performed using cumulative incidence analysis and multistate model analysis. For the cumulative incidence analysis, the achievement of the healed stage (stage 3) was considered as an event, and the impact of independent variables was checked by applying the Gray's test. In addition, a multivariate Cox model was performed to study the effect of different variables on the healing process.

A linear regression model was created to study the relationship of continuous variables (i.e., "minimum plastic thickness," "thickness with enhancement," and "brain sagging") with the time elapsed since the date of surgery. A logistic regression model was created to study the relationship of the categorical variables (i.e., "visualization of the first and second layers," "enhancement of the first and second layers," "visualization of the third layer," and "visualization of the fat") with the elapsed time from the date of surgery. Through these models, the influence of relevant clinical information, such as the type of radiotherapy and the use of a local flap, was analyzed.

The level of significance was 0.05 for all applied tests.

4 | Results

The study included 173 patients. General characteristics of the cohort are summarized in Table 1. One hundred and thirty-one patients were males (75.7%) and 42 females (24.3%), with a mean age at surgery of 62 years (95% confidence interval [95% CI]: 49.2–74.8). Fifty-two (30.0%) patients were smokers, and 54 (31.2%) had comorbidities, including 15 (8.7%) patients with diabetes mellitus, 14 (8.1%) with peripheral vascular disease, and 9 (5.2%) with chronic rhinosinusitis. ASB reconstruction was performed with three layers of ITT in 163 (94.2%) cases, while collagen matrix was used in 10 (5.8%) cases in place of the first (intradural) and second (epidural) ITT layer. Autologous adipose tissue was placed between the second and third layer in 154 (89.0%) cases. A local mucoperiosteal flap (i.e., septal flip flap) [18] was harvested to cover the dural reconstruction in 55 (31.8%) patients. One hundred and twenty-nine (74.6%) patients received adjuvant radiotherapy (RT), out of which 112 (86.8%) underwent RT alone and 17 (13.2%) chemoradiation. A total of 110 (63.6%) and 19 (11.0%) patients underwent photon-based intensity-modulated RT (IMRT) and intensity-modulated proton therapy (IMPT), respectively.

4.1 | Endoscopic Evaluation of the Healing Process

The following findings were extracted from 1097 follow-up endoscopies in 133 patients. General characteristics of this subcohort

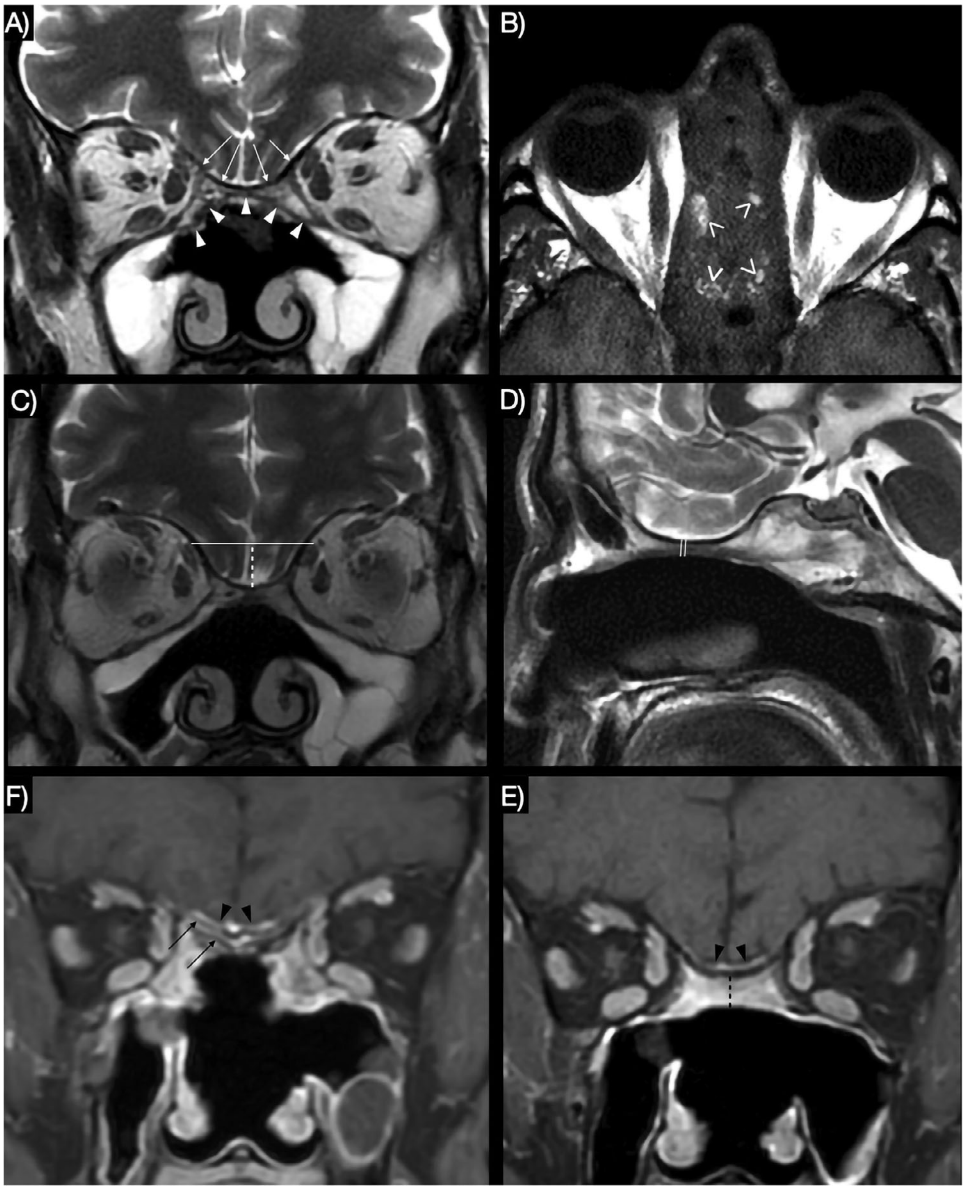

FIGURE 2 | Radiological features evaluated on post-operative MRI. In (A) the first and second layers of the iliotibial tract are visible and appear on this T2-weighted sequence as a hypointense intracranial layer (white arrows). The third layer is also identifiable, showing a hypointense signal on T2-weighted imaging and an extracranial location (white arrowheads). In (B), adipose tissue is visible on T1-weighted imaging, where it appears hyperintense and shows signal loss on fat-suppressed sequences. In (C), the brain sagging (white dotted line) is evaluated in the coronal plane passing through the origin of the optic nerves, using as a reference the line tangent to the upper margins of the superior oblique muscles (white line). (D) Minimum thickness of the ASB reconstruction, measured on the sagittal plane (white lines). Finally, a comparison is shown between MRI performed at 3 months after surgery (E) and at 12 months (F). In both examinations, contrast enhancement is observed on the dural side of the first layer (black arrowheads). However, on the 3-month MRI, the first and second layers are still distinguishable (black arrows) and no enhancing endonasal tissue is present. In contrast, on the 12-month MRI, enhancing endonasal tissue is visible (black dotted line), indicating that the skull base is undergoing or has completed the process of revascularization of the reconstructive graft.

of patients are summarized in Table S1. Figure 3 displays the cumulative incidence of complete healing of ASB reconstruction (stage 3), which was achieved in 15.9% of patients at 6 months, 69.9% at 12 months, and 94.4% at 24 months. The distribution of patients across endoscopic healing stages at predefined follow-up intervals is summarized in Table 2.

Inter-rater agreement for endoscopic assessment of ASB reconstruction healing was excellent. Overall reliability assessed using Krippendorff's alpha was 0.93. Pairwise weighted Cohen's kappa coefficients demonstrated substantial to almost perfect agreement across all rater combinations, with kappa values ranging from 0.756 to 0.870 (all $p < 0.001$, Table S2). Intra-rater agreement was also excellent, with a weighted Cohen's kappa of 0.942 ($p < 0.001$), indicating high consistency of repeated evaluations. Results of the uni- and multivariable analysis of factors potentially impacting the healing process are shown in Table 3. At the univariate analysis, age, diabetes, peripheral vascular

TABLE 1 | Main clinical features of the 173 patients included in the radiological analysis.

Characteristics		No. of patients (%) or means (CI)
Age at surgery (years)		62 (49.2, 74.8)
Gender	Males	131 (75.7%)
	Females	42 (24.3%)
Diabetes	Yes	15 (8.7%)
	No	158 (91.3%)
Smoking	Yes	52 (30.0%)
	No	121 (70.0%)
Peripheral vascular diseases	Yes	14 (8.1%)
	No	159 (91.9%)
Chronic rhinosinusitis	Yes	9 (5.2%)
	No	164 (94.8%)
Exposure to occupational risk factors	Yes	85 (49.1%)
	No	88 (50.9%)
Presentation	Primary	163 (94.2%)
	Recurrence	10 (5.8%)
Previous RT	Yes	9 (5.2%)
	No	164 (94.8%)
Previous CT	Yes	5 (2.9%)
	No	168 (97.1%)
Laterality of resection	Unilateral	49 (28.3%)
	Bilateral	124 (71.7%)
Margin status	R0	142 (82.1%)
	R1	31 (17.9%)
Reconstruction	Graft	173 (100%)
	Graft + local flap	55 (31.8%)
Adjuvant RT	No	44 (25.4%)
	IMRT	110 (63.6%)
	IMPT	19 (10.1%)
Histology	ITAC	104 (60.1%)
	nITAC	6 (3.5%)
	SCC	3 (1.7%)
	ONB	36 (20.8%)
	MM	5 (2.9%)
	AdCC	3 (1.7%)
	NUT carcinoma	1 (0.6%)
	MANEC	1 (0.6%)
	SNUC	5 (2.9%)
	NEC	2 (1.2%)
	MiNEN	2 (1.2%)
	Sarcoma[a]	4 (2.3%)
Carcinoma NOS	1 (0.6%)	
pT	pT1	13 (7.5%)
	pT2	46 (26.6%)
	pT3	52 (30.1%)
	pT4a-4b	62 (35.8%)
FU (months)		24.5 (6.0, 43.0)

Abbreviations: AdCC: adenoid cystic carcinoma; CI: confidence interval; IMPT: intensity-modulated proton therapy; IMRT: intensity-modulated radiation therapy; ITAC: intestinal type adenocarcinoma; MANEC: mixed adeno-neuroendocrine carcinoma; MiNEN: mixed neuroendocrine non-neuroendocrine neoplasms; MM: mucosal melanoma; NEC: sinonasal neuroendocrine carcinoma; nITAC: non intestinal type adenocarcinoma; ONB: olfactory neuroblastoma; SCC: squamous cell carcinoma; SNUC: sinonasal undifferentiated carcinoma.

[a]Ewing, myofibroblastic, and biphenotypic sinonasal sarcomas.

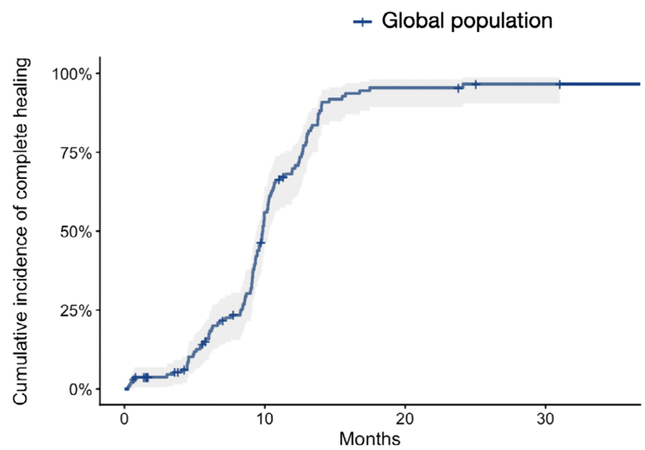

FIGURE 3 | Complete healing cumulative incidence plot in the overall series.

disease, smoking, and previous treatments considered separately (surgery, RT, or chemotherapy) did not affect the healing process. Female gender, chronic rhinosinusitis, recurrent presentation of the disease, only graft-based (i.e., with no flap) reconstruction, adjuvant RT, bilateral defect, and positive margins were found to negatively impact the healing process. The following variables were included in the multivariable analysis: age at surgery, use of flap, adjuvant RT, and margin status. In this analysis, the use of a local flap and adjuvant RT maintained statistical significance while age and margin status did not. Figure 4 illustrates the cumulative incidence of complete healing of ASB reconstructions according to adjuvant RT. Pairwise comparisons showed a significantly lower incidence of complete healing in patients treated with IMPT compared with IMRT ($p = 0.004$) and with no adjuvant RT ($p = 0.003$), while no significant difference was observed between IMRT and no RT ($p = 0.246$). The use of a local pedicled flap was associated with a significantly higher probability of achieving complete healing over time compared with reconstruction without a flap (Figure 5; Gray's test, $p <$

TABLE 2 | Distribution of patients across different endoscopic healing stages and phases of anterior skull base reconstruction at predefined postoperative timepoints.

Stage	Phase	6 months		12 months		24 months	
1 (postop)	1	0 (0%)		0 (0%)		0 (0%)	
2 (healing)	2	112 (84.2%)	7 (5.3%)	50 (37.6%)	2 (1.5%)	22 (16.5%)	2 (1.5%)
	3		46 (34.6%)		15 (11.3%)		10 (7.5%)
	4		59 (44.3%)		33 (24.8%)		10 (7.5%)
3 (healed)	5	21 (15.8%)	13 (9.8%)	83 (62.4%)	48 (36.1%)	111 (83.5%)	20 (15.0%)
	6		8 (6.0%)		35 (26.3%)		91 (68.5%)

Note: Values are reported as number of patients who reached and did not progress beyond the corresponding healing stage/phase within each time interval. Patients who progressed to a more advanced healing stage/phase within the same interval were not counted in the corresponding category.

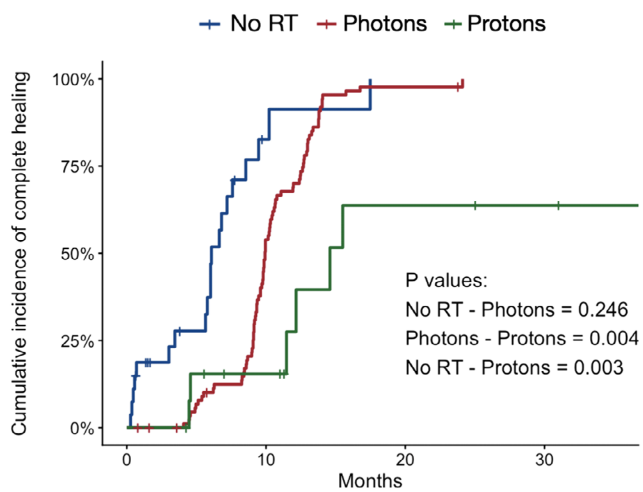

FIGURE 4 | Complete healing cumulative incidence plot in patient that did not undergo adjuvant RT (0), and in patients that underwent adjuvant photon-RT (F) and proton-RT (P).

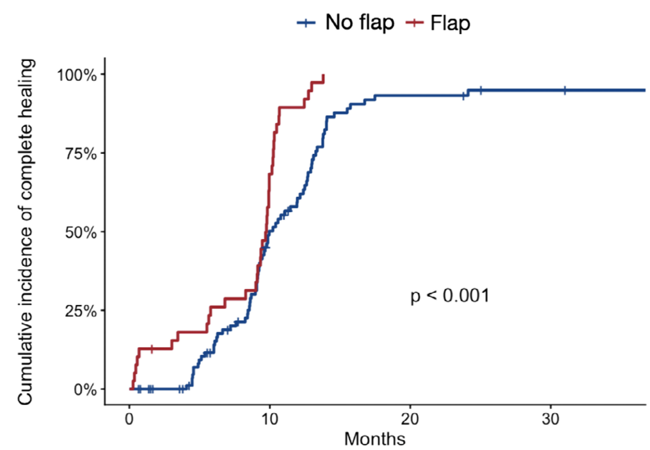

FIGURE 5 | Complete healing cumulative incidence plot in patient that did not undergo surgery with a flap (0), and in patients that underwent surgery with a local flap (1).

0.001). Table 4 summarizes the cumulative incidence of complete healing at 12 months in the different sub-cohorts of patients.

4.2 | Radiological Evaluation of the Healing Process

All 173 patients were included in the radiological analysis, based on a total of 832 MRIs. The mean time interval between surgery and the first postoperative MRI (baseline) was 5.97 months (95% CI, 5.47–6.48), with a median of 5.36 months (IQR, 4.53–6.25). The first and second ITT layers were consistently visible, whereas adipose tissue and the third ITT layer showed a progressive reduction in visibility over time ($p < 0.001$).

Longitudinal radiological changes in the overall cohort and subgroup analyses according to adjuvant RT modality and use of local flaps are summarized in Table 5, while model-based predicted values at predefined follow-up intervals are reported in Table 6. The temporal trends of minimum reconstruction thickness and brain sagging are graphically illustrated in Figure 6A,B, respectively. The mean minimum thickness of the ASB reconstruction significantly decreased over time (−0.96 mm/year, $p < 0.001$), with a clear attenuation of the reduction rate at longer follow-up, stabilizing around 4–5 mm, as shown in Figure 6A. Thickness reduction was significant in patients without adjuvant RT and in those treated with IMRT, while no significant change was observed in the IMPT subgroup. Reconstructions performed with a local flap did not show a significant thickness reduction, whereas those without a flap did. Endonasal enhancement thickness progressively decreased over time, with lower baseline values and faster reduction rates in irradiated patients. In contrast, reconstructions using a local flap showed greater baseline enhancement and relative stability over time. Brain sagging increased significantly during follow-up (0.72 mm/year, $p < 0.001$), with a tendency toward stabilization at longer intervals, with values clustering around approximately 5–6 mm, as illustrated in Figure 6B. This increase was more pronounced in patients receiving adjuvant IMRT, whereas no significant change was observed in the IMPT group.

5 | Discussion

ASB reconstruction after TES for malignant tumors is a safe procedure [3, 4, 8, 12], but data regarding the time course of reconstruction healing and the factors influencing this process remain limited. The present multicentric retrospective study was

TABLE 3 | Univariate and multivariate analysis on different variables with potential effect on the healing process.

		Univariate analysis		Multivariate analysis	
Variable	**Transition**[a]	**HR (95% CI)**	***p* value**	**HR (95% CI)**	***p* value**
Male gender (ref. female)	1	2.20 (1.40, 3.45)	**< 0.001**		
	2	1.67 (0.45, 6.23)	0.441		
	3	0.91 (0.58, 1.43)	0.696		
Age	1	1.09 (0.95, 1.25)	0.217	1.09 (0.95, 1.26)	0.223
	2	1.00 (0.80, 1.26)	0.976	1.16 (0.78, 1.73)	0.460
	3	1.04 (0.90, 1.21)	0.583	1.09 (0.93, 1.28)	0.272
Diabetes (ref. no diabetes)	1	1.03 (0.52, 2.03)	0.934		
	3	0.90 (0.42, 1.95)	0.800		
Peripheral vascular diseases (ref. no peripheral vascular diseases)	1	1.10 (0.58, 2.11)	0.769		
	3	0.99 (0.48, 2.06)	0.998		
Chronic rhinosinusitis (ref. no chronic rhinosinusitis)	1	3.56(1.11, 11.44)	**0.033**		
	3	1.15 (0.28, 4.69)	0.846		
Smoking (ref. no smoking)	1	0.96 (0.66, 1.40)	0.836		
	2	1.94 (0.49, 7.67)	0.344		
	3	0.8 (0.02, 0.08)	0.370		
Recurrence presentation (ref. primary presentation)	1	0.93 (0.45, 1.90)	0.838		
	3	4.04 (1.58, 10.32)	**0.003**		
Flap (ref. no flap)	1	0.99 (0.88, 1.12)	0.940	1.03 (0.91, 1.17)	0.598
	2	1.49 (1.01, 2.21)	**0.045**	1.96 (0.99, 3.83)	**0.050**
	3	1.20 (1.06, 1.35)	**0.004**	1.16 (1.02, 1.32)	**0.022**
Adjuvant RT with photons (ref. no RT)	1	0.48 (0.30, 0.75)	**0.001**	0.48 (0.29. 0.78)	**0.003**
	3	0.44 (0.26, 0.75)	**0.002**	0.40 (0.22, 0.71)	**0.001**
Adjuvant RT with protons (ref. no RT)	1	1.11 (0.57, 2.15)	0.756	0.97 (0.45, 2.10)	0.940
	3	0.12 (0.05, 0.30)	**< 0.001**	0.15 (0.05, 0.45)	**< 0.001**
Bilateral defect (ref. unilateral defect)	1	0.99 (0.68, 1.42)	0.962		
	3	0.65 (0.44, 0.97)	**0.033**		
Previous RT	1	1.88 (0.87, 4.07)	0.106		
	3	1.13 (0.41, 3.08)	0.813		
Previous CT	1	1.01 (0.40, 2.52)	0.981		
	3	1.05 (0.33, 3.35)	0.928		
Previous surgery	1	0.99 (0.43, 2.29)	0.994		
	3	2.02 (0.73, 5.60)	0.175		
R1 (ref. R0)	1	1.58 (1.00, 2.48)	**0.049**	1.18 (0.68, 2.04)	0.559
	3	0.38 (0.19, 0.74)	**0.004**	0.68 (0.31, 1.48)	0.332

Note: Hazard ratio (HR) indicates the probability of transition occurring associated with the variable. Values in bold indicate statistical significance ($p < 0.05$).
Abbreviations: CI: confidence interval; HR: hazard ratio.
[a]Data inherent in transition 2 cannot be reported due to failure of the statistical model to converge for the following variables: diabetes, peripheral vasculopathy, chronic rhinosinusitis, presentation, adjuvant radiotherapy, bilaterality of defect, prior radiotherapy, prior chemotherapy, prior surgery, and surgical margins.

designed with the primary intent of defining the time to complete healing of ASB reconstruction. To be as objective as possible in assessing the healing of the reconstruction, we first designed an endoscopic classification of the healing process. The classification includes six phases and reflects the physiological integration process of ITT in the ASB. It is assumed that the graft acts as a scaffold for the migration of fibroblasts from the dural margins, until it is replaced by connective tissue [5, 12]. A similar process is surmised for collagen matrix-based grafts [21]. On the endonasal side, the third layer of ITT necrotizes in a short time in most cases, and when the healing process starts, its margins are progressively replaced by granulation tissue. Integration of the third layer is

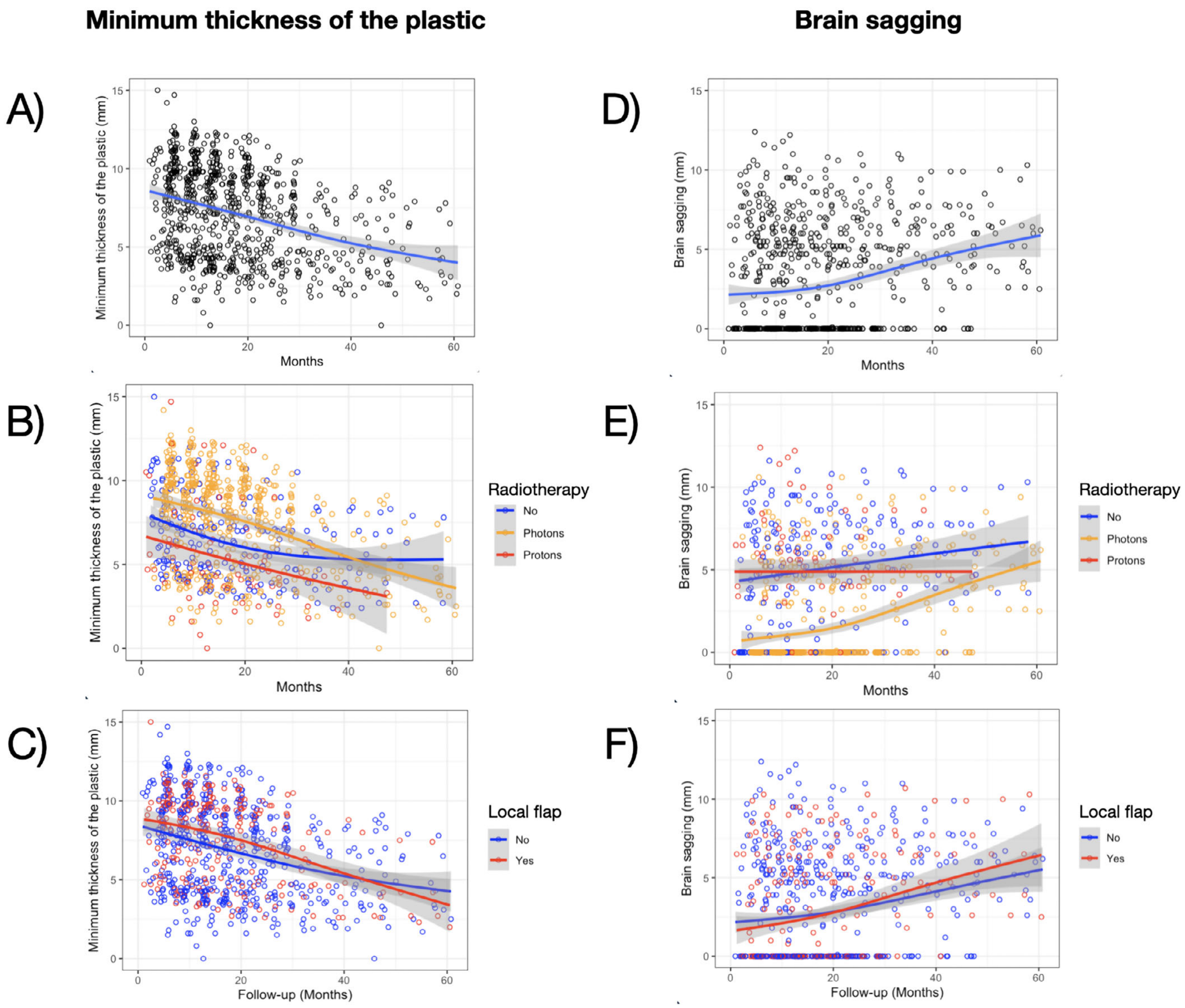

FIGURE 6 | Longitudinal changes in minimum plasty thickness and brain sagging. Scatter plots showing the relationship between follow-up time (months) and minimum plasty thickness (A–C) and brain sagging (D–F). Lines represent fitted regression curves with 95% confidence intervals. Panels (B)–(E) are stratified by radiotherapy and Panels (C)–(F) by local flap reconstruction.

TABLE 4 | cumulative incidence of complete healing (achievement of Grades 5 and 6) at 12 months in patients that underwent adjuvant RT (radiotherapy) or not, and in patients were a local pedicled flap (i.e., septal flip flap) was used or not in the reconstruction.

Characteristic	12-month cumulative incidence	*p*-value
Adjuvant RT		
No RT	91.3%	0.084
Photons	70.0%	
Protons	27.5%	
Flap		
No flap	60.7%	**< 0.001**
Flap	89.4%	

Note: Values in bold indicate statistical significance ($p < 0.05$).

rarely observed, supporting its role as a temporary protective layer for the underlying adipose tissue and ITT layers. Granulation tissue progresses in a centripetal fashion until it completely coats the ASB and is subsequently replaced by mucosa with a similar centripetal pattern.

The proposed classification enabled a dynamic assessment of healing, showing a predominantly unidirectional progression through stages, with variable timing across patients. Delayed transitions and persistence in intermediate stages were more frequent in patients undergoing adjuvant RT or without a local flap, suggesting an effect on healing kinetics. Radiological findings complemented endoscopic evaluation by documenting the structural evolution of the reconstruction. Progressive reduction in adipose tissue and outer ITT visibility, along with preservation of deeper layers, support a process of resorption and fibrous replacement over a stable scaffold. Decreasing reconstruction thickness and increasing brain sagging, both tending to sta-

TABLE 5 | longitudinal changes in radiological parameters of anterior skull base (ASB) reconstruction. Linear regression models were used to estimate baseline values and annual rates of change in the overall cohort and across predefined subgroups according to adjuvant radiotherapy (RT) modality (IMRT = intensity modulated RT; IMPT = intensity modulated proton therapy) and use of local flaps.

Outcome variable	Subgroup	Baseline estimate (mm)	Annual rate of change (mm/year)	*p* value
ASB reconstruction minimum thickness	Overall cohort	8.58	−0.96	< 0.001
	No adjuvant RT	7.44	−0.60	< 0.001
	IMRT	9.34	−1.08	**0.007**
	IMPT	6.87	−1.08	0.227
	No local flap	8.26	−0.84	**< 0.001**
	Local flap	9.25	−0.36	0.215
Endonasal enhancement thickness	Overall cohort	2.20	−0.108	**0.003**
	No adjuvant RT	2.92	−0.36	**< 0.001**
	IMRT	2.01	−0.84	**< 0.001**
	IMPT	1.22	−0.84	**0.003**
	No local flap	1.97	−0.108	**0.012**
	Local flap	2.58	0.06	0.4872
Brain sagging	Overall cohort	1.64	0.72	**< 0.001**
	No adjuvant RT	4.24	0.48	**0.001**
	IMRT	0.10	0.96	**0.018**
	IMPT	4.90	0.00	0.214
	No local flap	1.81	0.72	**< 0.001**
	Local flap	1.23	1.08	0.159
Visibility of first and second layers	Overall cohort	99.3	−0.12	0.726
	No adjuvant RT	99.9	0.00	1.000
	IMRT	98.9	−0.12	1.000
	IMPT	100	0.00	1.000
	No local flap	98.8	−0.60	0.832
	Local flap	99.9	+0.12	1.000
Visibility of fat tissue	Overall cohort	28.9	−14,4	**< 0.001**
	No adjuvant RT	44.5	−0.48	**0.003**
	IMRT	22.6	−0.60	0.454
	IMPT	71.7	−2,16	**0.014**
	No local flap	30.1	−0.72	**< 0.001**
	Local flap	26.9	−0.36	0.151
Visibility of third layer	Overall cohort	51.9	−0.6	**< 0.001**
	No adjuvant RT	60.8	−0.48	**0.001**
	IMRT	50.6	−0.72	0.093
	IMPT	67.4	−1.68	**0.022**
	No local flap	56.3	−1.56	**< 0.001**
	Local flap	73.3	−0.24	**< 0.001**
Enhancement of the first and second layers	Overall cohort	94.3	−0.24	**0.043**
	No adjuvant RT	86.6	−0.24	**0.075**
	IMRT	97.7	−0.24	0.983
	IMPT	84.3	0.60	0.170
	No local flap	94.3	0.60	**0.083**
	Local flap	92.7	−0.60	**< 0.001**

Note: Values in bold indicate statistical significance ($p < 0.05$).

TABLE 6 | Predicted values of radiological parameters of anterior skull base (ASB) reconstruction at predefined postoperative time points. Model-based estimates derived from linear regression analyses are reported for minimum reconstruction thickness, endonasal enhancement thickness, and brain sagging at baseline and at 12, 24, 36, and 60 months after surgery.

Outcome variable (mm)	12 months	24 months	36 months	60 months
Minimum thickness	7.61	6.63	5.66	3.71
Endonasal enhancement	2.09	1.97	1.86	1.63
Brain sagging	2.42	3.19	3.97	5.52

bilize over time, likely reflect physiological remodeling and intracranial adaptation. These changes were more pronounced in IMRT-irradiated patients and less evident in reconstructions with local flaps, indicating a role of vascularized tissue in maintaining structural stability. These observations provide a reference framework for the expected radiological evolution of ASB reconstructions, potentially helping clinicians distinguish physiological postoperative remodeling from abnormal findings during routine oncological surveillance.

In this study, we identified six variables negatively affecting the healing process of the ASB reconstructions: only graft-based reconstruction (i.e., no use of local flaps), adjuvant RT, recurrent presentation of the disease, involved margins, male gender, and chronic rhinosinusitis. In the literature, factors such as diabetes, peripheral vascular disease, and smoking are considered risk factors, as they create an endothelial dysfunction that reduces the integration of skull-base reconstructions; [22] conversely, our results did not support this hypothesis.

The advantages of local flaps are reported in the literature and include excellent success rates and rapid healing of the surgical cavity with reduced crusting and nasal discharge [9, 12, 18, 23]. However, no previous studies have quantified the benefits in terms of healing of the surgical site. In our study, both uni- and multivariable analysis confirmed the importance of local flaps in promoting faster healing of the reconstruction. At 12 months, 89.4% of patients who underwent reconstruction with a local flap achieved a complete healing stage, compared with 60.7% of patients in whom a local flap was not used. However, their use requires careful consideration when dealing with sinonasal cancers in order not to transgress oncological principles. It should also be acknowledged that regional flaps, such as the pericranial flap and the temporoparietal fascia flap, were not included in the present analysis because they were selectively used in a limited number of salvage or complex cases, precluding meaningful statistical evaluation. Moreover, since these flaps are entirely connective tissue-based, they may be associated with slower healing kinetics, as endonasal surface re-epithelialization occurs by secondary intention.

Adjuvant RT and its effects on the healing process have been analyzed in several studies with different outcomes. Turri-Zanoni et al. did not find any significant association between adjuvant RT and post-operative complications [12]. Differently, Zanation et al. showed a relationship between RT and skull base reconstruction failures and stated that patients who underwent adjuvant IMPT are at higher risk for reconstruction failure (i.e., CSF leak). In an interesting study conducted on 152 cases by Thorp et al. [16], 37 patients received adjuvant RT and no significant correlation was found between perioperative complication rates and RT; however, an increased risk of prolonged (>6 months) skull base crusting was found. Our results are in line with this observation: both adjuvant IMRT and IMPT reduced the probability of achieving complete endoscopic healing. This was particularly evident in the IMPT cohort, where a consistent number of patients was still undergoing the healing process at the end of the observation (Figure 4). Adjuvant IMRT appeared to influence the healing process also in the radiological analysis, being associated with greater reductions in minimum thickness of the reconstruction over time, decreased vascularized endonasal tissue, and increased brain sagging.

Exposure to RT leads to a chronically increased level of inflammatory cytokines, including IL-1, TNF-α, and IFN-γ, which play a pivotal role in chronic oxidative damage [24]. The relationship between chronic inflammation and oxidative damage after RT can explain why some patients would not completely heal. IMPT appears to further delay the healing process. This finding may be attributed to the physical properties of protons, which are generally assumed to have a relative biological effectiveness of approximately 1.1 compared with photons, along with greater dose conformality and sharper dose fall-off, which consequently overlaps with the reconstruction site. In IMRT, the proximity of organs at risk, such as the optic nerves and brain, may constrain the dose received by the reconstruction. IMPT instead allows a more precise and conformal delivery of the radiation dose [25]. Considering the position of reconstruction relative to the gross tumor volume of nasoethmoidal cancers, it becomes clear that ASB reconstruction is likely to receive the maximum delivered dose with adjuvant IMPT. Further analyses assessing dose distribution and inhomogeneity in the irradiated volume in patients receiving adjuvant RT (according to RT modalities) for a sinonasal cancer are warranted to explore this hypothesis and potentially assist in optimizing the biological impact of the radiation (or tailoring the energy deposition) specifically within the reconstruction site.

This study is limited by its retrospective design, which may introduce selection bias and preclude causal inferences. The proposed endoscopic healing classification has not yet been externally validated and was applied retrospectively, potentially introducing additional bias. In addition, the allocation of adjuvant RT modality (IMRT vs. IMPT) was not randomized, introducing an inherent selection bias, as patients treated with IMPT generally presented with more critical tumor extensions and a higher risk of toxicity to adjacent organs at risk. Furthermore, detailed data regarding the dose delivered to the reconstruction site were not available. Therefore, the observed association between IMPT and delayed healing should be interpreted with caution and cannot be assumed to reflect a causal effect of proton therapy itself. Finally, although based on the same follow-up protocol, MRI follow-up intervals were not strictly uniform, which may have affected the accuracy of radiological temporal analyses.

6 | Conclusions

In this multicentric retrospective study, adjuvant RT and the use of vascularized flaps were identified as key factors influencing the healing of ASB reconstructions after ERTC. Adjuvant RT, particularly IMPT, was associated with delayed achievement of endoscopic consolidated healing, whereas the use of flaps was associated with improved healing outcomes. Importantly, our findings indicate that complete healing frequently requires substantially longer time than commonly assumed, often extending beyond 12 months. This information should be taken into account during preoperative patient counseling and when planning postoperative surveillance. These findings indicate that, in patients with a high likelihood of requiring adjuvant RT (especially IMPT), the inclusion of vascularized tissue in the reconstructive strategy should be carefully considered. In selected cases, the potential use of a local (e.g., inferior turbinate/lateral nasal wall) or regional flap (e.g., pericranial/temporoparietal fascia flap) may also be considered as part of the reconstructive planning, although this hypothesis warrants further investigation.

Acknowledgments

Open access publishing facilitated by Universita degli Studi di Padova, as part of the Wiley - CRUI-CARE agreement.

Funding

The authors have nothing to report.

Conflicts of Interest

The authors declare no conflicts of interest.

References

1. P. Nicolai, P. Battaglia, M. Bignami, et al., "Endoscopic Surgery for Malignant Tumors of the Sinonasal Tract and Adjacent Skull Base: A 10-Year Experience," *American Journal of Rhinology* 22, no. 3 (2008): 308–316, https://doi.org/10.2500/ajr.2008.22.3170.

2. P. Castelnuovo, P. Battaglia, M. Turri-Zanoni, et al., "Endoscopic Endonasal Surgery for Malignancies of the Anterior Cranial Base," *World Neurosurgery* 82, no. S6 (2014): S22–S31, https://doi.org/10.1016/j.wneu.2014.07.021.

3. D. Mattavelli, M. Ferrari, A. Bolzoni Villaret, et al., "Transnasal Endoscopic Surgery in Selected Nasal-Ethmoidal Cancer With Suspected Brain Invasion: Indications, Technique, and Outcomes," *Head & Neck* 41, no. 6 (2019): 1854–1862, https://doi.org/10.1002/hed.25621.

4. D. Mattavelli, A. Schreiber, M. Ferrari, et al., "Three-Layer Reconstruction With Iliotibial Tract After Endoscopic Resection of Sinonasal Tumors," *World Neurosurgery* 101 (2017): 486–492, https://doi.org/10.1016/j.wneu.2017.02.066.

5. B. Schick, R. Ibing, D. Brors, and W. Draf, "Long-Term Study of Endonasal Duraplasty and Review of the Literature," *Annals of Otology, Rhinology and Laryngology* 110, no. 2 (2001): 142–147, https://doi.org/10.1177/000348940111000209.

6. A. B. Villaret, A. Schreiber, P. Battaglia, and M. Bignami, "Endoscopy-Assisted Iliotibial Tract Harvesting for Skull Base Reconstruction: Feasibility on a Cadaveric Model," *Skull Base: Official Journal of the North American Skull Base Society* 21, no. 3 (2011): 185–188, https://doi.org/10.1055/s-0031-1275260.

7. G. Bertazzoni, A. Vinciguerra, D. Camous, et al., "Morbidity of Multimodal Treatments Including Endoscopic Surgery for Sinonasal Malignancies: Results of an International Collaborative Study on 940 Patients (MUSES)," *Head & Neck* 47, no. 1 (2025): 371–385, https://doi.org/10.1002/hed.27916.

8. D. Mattavelli, A. Schreiber, A. B. Villaret, et al., "Complications and Donor Site Morbidity of 3-Layer Reconstruction With Iliotibial Tract of the Anterior Skull Base: Retrospective Analysis of 186 Patients," *Head & Neck* 40, no. 1 (2018): 63–69, https://doi.org/10.1002/hed.24931.

9. G. Bozkurt, F. Leone, A. D. Arosio, et al., "Septal Flip Flap for Anterior Skull Base Reconstruction After Endoscopic Transnasal Craniectomy: Long-Term Outcomes," *World Neurosurgery* 128 (2019): e409–e416, https://doi.org/10.1016/j.wneu.2019.04.166.

10. A. B. Kassam, A. Thomas, R. L. Carrau, et al., "Endoscopic Reconstruction of the Cranial Base Using a Pedicled Nasoseptal Flap," *Neurosurgery* 63, no. S1 (2008): ONS44–52, discussion ONS52-53, https://doi.org/10.1227/01.neu.0000297074.13423.f5.

11. C. L. Gruss, M. Al Komser, and M. K. Aghi, "Risk Factors for Cerebrospinal Leak After Endoscopic Skull Base Reconstruction With Nasoseptal Flap," *Otolaryngology–Head and Neck Surgery: Official Journal of the American Academy of Otolaryngology-Head and Neck Surgery* 151, no. 3 (2014): 516–521, https://doi.org/10.1177/0194599814536688.

12. M. Turri-Zanoni, J. Zocchi, A. Lambertoni, et al., "Endoscopic Endonasal Reconstruction of Anterior Skull Base Defects: What Factors Really Affect the Outcomes?," *World Neurosurgery* 116 (2018): e436–e443, https://doi.org/10.1016/j.wneu.2018.04.225.

13. M. R. Patel, M. E. Stadler, C. H. Snyderman, et al., "Endoscopic Skull Base Reconstructive Options and Limitations," *Skull Base: Official Journal of the North American Skull Base Society* 20, no. 6 (2010): 397–404, https://doi.org/10.1055/s-0030-1253573, How to choose?.

14. E. Soudry, J. H. Turner, J. V. Nayak, and P. H. Hwang, "Acta Otorhinolaryngologica Italica: Organo Ufficiale della Società Italiana di Otorinolaringologia e Chirurgia Cervico-Facciale," *Otolaryngology–Head and Neck Surgery: Official Journal of the American Academy of Otolaryngology–Head and Neck Surgery* 150, no. 5 (2014): 730–738, https://doi.org/10.1177/0194599814520685.

15. R. J. Harvey, P. Parmar, R. Sacks, and A. M. Zanation, "Endoscopic Skull Base Reconstruction of Large Dural Defects: A Systematic Review of Published Evidence," *Laryngoscope* 122, no. 2 (2012): 452–459, https://doi.org/10.1002/lary.22475.

16. B. D. Thorp, S. B. Sreenath, C. S. Ebert, and A. M. Zanation, "Endoscopic Skull Base Reconstruction: A Review and Clinical Case Series of 152 Vascularized Flaps Used for Surgical Skull Base Defects in the Setting of Intraoperative Cerebrospinal Fluid Leak," *Neurosurgical Focus* 37, no. 4 (2014): E4, https://doi.org/10.3171/2014.7.FOCUS14350.

17. A. M. Zanation, R. L. Carrau, C. H. Snyderman, et al., "Nasoseptal Flap Reconstruction of High Flow Intraoperative Cerebral Spinal Fluid Leaks During Endoscopic Skull Base Surgery," *American Journal of Rhinology and Allergy* 23, no. 5 (2009): 518–521, https://doi.org/10.2500/ajra.2009.23.3378.

18. P. Battaglia, M. Turri-Zanoni, F. De Bernardi, et al., "Septal Flip Flap for Anterior Skull Base Reconstruction After Endoscopic Resection of Sinonasal Cancers: Preliminary Outcomes," *Acta Otorhinolaryngologica*

Italica: Organo Ufficiale della Società Italiana di Otorinolaringologia e Chirurgia Cervico-Facciale 36, no. 3 (2016): 194–198, https://doi.org/10.14639/0392-100X-748.

19. A. El-Naggar, J. Chan, J. Grandis, T. Takata, and P. Slootweg, *WHO Classification of Head and Neck Tumours* (2017).

20. J. Brierley, M. Gospodarowicz, and C. Wittekind, *TNM Classification of Malignant Tumours*, 8th ed. (Wiley-Blackwell, 2017).

21. P. K. Narotam, S. José, N. Nathoo, C. Taylon, and Y. Vora, "Collagen Matrix (DuraGen) in Dural Repair: Analysis of a New Modified Technique," *Spine* 29, no. 24 (2004): 2861–2867, discussion 2868–2869, https://doi.org/10.1097/01.brs.0000148049.69541.ad.

22. K. Kim, A. M. S. Ibrahim, P. G. L. Koolen, N. Seyidova, and S. J. Lin, "Analysis of Morbidity and Mortality in Patients Undergoing Skull Base Reconstruction," *Journal of Craniofacial Surgery* 26, no. 1 (2015): 135–140, https://doi.org/10.1097/SCS.0000000000001399.

23. E. D. McCoul, V. K. Anand, A. Singh, G. G. Nyquist, M. R. Schaberg, and T. H. Schwartz, "Long-Term Effectiveness of a Reconstructive Protocol Using the Nasoseptal Flap After Endoscopic Skull Base Surgery," *World Neurosurgery* 81, no. 1 (2014): 136–143, https://doi.org/10.1016/j.wneu.2012.08.011.

24. R. Yahyapour, P. Amini, S. Rezapour, et al., "Radiation-induced Inflammation and Autoimmune Diseases," *Military Medical Research* 5 (2018): 9, https://doi.org/10.1186/s40779-018-0156-7.

25. J. K. Kim, J. E. Leeman, N. Riaz, S. McBride, C. J. Tsai, and N. Y. Lee, "Proton Therapy for Head and Neck Cancer," *Current Treatment Options in Oncology* 19, no. 6 (2018): 28, https://doi.org/10.1007/s11864-018-0546-9.

Supporting Information

Additional supporting information can be found online in the Supporting Information section.

Supporting File 1: alr70232-sup-0001-SuppMat.docx **Supporting File 2**: alr70232-sup-0002-eTables.docx